Isotope effects on direct and indirect processes of hydrogen abstraction from Cu(111)

Isotope effects on direct and indirect processes of hydrogen abstraction from Cu(111)

Yoshio Miura[1]**, Hideaki Kasai**[1] **and Wilson Agerico Diño**[1,2]

[1] Department of Applied Physics, Osaka University, Suita, Osaka 565-0871, Japan
[2] Institute of Industrial Science, The University of Tokyo, Komaba, Meguro-ku, Tokyo 153-8505, Japan

E-mail: miura@dyn.ap.eng.osaka-u.ac.jp

Abstract
We investigate and discuss isotope effects on hydrogen abstraction from Cu(111) by performing quantum dynamics calculations that consider both direct (an impinging hydrogen atom directly abstracts an adsorbed hydrogen atom) and indirect (the impinging hydrogen atom diffuses across the surface before it abstracts an adsorbed hydrogen atom) processes quantum mechanically. Our calculation results show that the abstraction reaction probabilities P_{reac} are 0.742(D-on-D) > 0.640(H-on-D) > 0.594(H-on-H) > 0.533(D-on-H). (Note that the term 'X-on-Y' indicates abstraction of Y atoms adsorbed on the surface by gas-phase X atoms.) Furthermore, the mean normal translational and vibrational energies for H-on-D are larger than those for D-on-H, while the mean parallel translational energy for D-on-H is comparable with that for H-on-D. This implies that the decrease in the abstraction reaction probability for D-on-H, as compared with that for H-on-D, is mainly due to the decrease in the frequency of occurrence of the direct process in abstraction reactions.

1. Introduction

Reactions of gas-phase hydrogen atoms with other hydrogen atoms adsorbed on metal and semiconductor surfaces have attracted much attention in recent years. Because they are fundamentally important for understanding the mechanism of complex chemical reactions occurring on solid surfaces (e.g., synthesis of organic compounds from gas-phase CO_2 on metal surfaces, etching in semiconductors, nuclear fusion, and so on). As one prototype of these reactions, abstraction of hydrogen atoms adsorbed on metal and semiconductor surfaces by gas-phase hydrogen atoms has been extensively investigated, theoretically, as well as experimentally. The results have usually been interpreted in terms of a *direct process/mechanism* (e.g., the Eley–Rideal (ER) reaction) in which incident hydrogen atoms directly react with adsorbed hydrogen atoms in a single collision. Rettner and Auerbach [1, 2]

experimentally investigated the abstraction of D (H) atoms adsorbed on Cu(111) by H (D) atoms impinging from gas-phase [D (H)(g) + H (D)(a)/Cu(111)]. Note that H (D)(a) and D (H)(g) correspond to D (H) atoms adsorbed on Cu(111) and H (D) atoms impinging from the gas phase, respectively. They demonstrated that due to the exothermicity of the reaction (∼2.6 eV), the translational, vibrational, and rotational motions of the product HD are highly excited, as compared to the motions of HD associatively desorbing from Cu(111). Quantum dynamics calculation of the abstraction for D (H)(g) + H (D)(a)/Cu(111) also suggested that the motions of the product HD are energetically excited, as observed in experiments [3, 4]. However, the theoretically estimated abstraction cross section (∼0.5 Å²) turned out to be smaller than that obtained in experiments (∼5 Å²) by one order of magnitude. Therefore, it was suggested that other pathways to the reaction, *indirect processes/mechanisms* (in which trapped D (H) atoms on the surface diffuse across the surface, e.g., as hot atoms (HA), and then react with other adsorbed H (D)), play an important role in the abstraction dynamics [5–19].

Many experimental [5–11] and theoretical [12–19] studies have been carried out in an effort to understand the dynamics and kinetics of direct and indirect processes, and to distinguish the direct and indirect processes by means of angular and/or energy distributions of product molecules. A clear experimental signature is the observation of a peculiar isotope effect. The kinetic energy of the desorbing HD molecules depends strongly on the choice of which isotope to use as the projectile in the incident beam, and which one to use as the target on the surface. Although isotope effects are theoretically investigated in previous classical and quantum dynamics calculations [12, 13, 17], to our knowledge, this is the first theoretical study of the isotope effects on hydrogen abstraction reactions in which both the direct and indirect processes are treated quantum mechanically in the dynamics calculations.

Our purpose here is to give a microscopic understanding of the dynamics of hydrogen abstraction reactions, and a quantum-mechanical clarification of the difference between the direct and indirect processes by analysing the dynamics of the product molecules. We report isotope effects on hydrogen abstraction from Cu(111) for a surface coverage $\Theta_H = 0.500$ monolayers (ML), which corresponds to 1.08×10^{14} atoms cm^{-2}. We perform quantum dynamics calculations which quantum mechanically include both the direct and indirect processes by using the numerically stable time-independent coupled-channel method [23, 25].

2. Theory

Here, we consider the reaction between an incident hydrogen atom and a target hydrogen atom initially adsorbed on a Cu(111) surface (the initial state). The incident atom either directly or indirectly abstracts the adsorbed atom, and the resulting hydrogen molecule desorbs from the surface (the final state).

In the experiments [2], the incident beams of hydrogen atoms were directed along the [1$\bar{2}$1] direction on the Cu(111), and the product hydrogen molecules were also detected (in the scattering plane) along the [1$\bar{2}$1] direction, with effective integration over all out-of-plane angles. Thus, as a first approximation, we are justified in including only one surface coordinate (to describe surface corrugation), as one of the dynamical variables in the present calculations. In this paper, since we will focus our investigation on the isotope effects on hydrogen abstraction reactions, we also drop the rotational degree of freedom from among the dynamical variables in our calculations. The corresponding model Hamiltonian in our system has the form

$$ H = -\frac{\hbar^2}{2\mu}\frac{\partial^2}{\partial r^2} - \frac{\hbar^2}{2M}\frac{\partial^2}{\partial Z^2} - \frac{\hbar^2}{2M}\frac{\partial^2}{\partial X^2} + \tilde{V}(r, Z, X), \tag{1} $$

where M is the total mass, and μ is the reduced mass of the two hydrogen atoms. X is the centre-of-mass coordinate of the two hydrogen atoms parallel to the surface, and Z is the centre-of-mass coordinate of the two hydrogen atoms normal to the surface. r is the relative distance of the two hydrogen atoms. $\tilde{V}(r, Z, X)$ is the corresponding potential energy surface (PES). In the present study, the interaction of the hydrogen atoms with each other and with Cu(111) is modelled by a London–Eyring–Polanyi–Sato (LEPS) potential [20]. Its application to the abstraction reactions on the corrugated surface has been described in detail earlier [14]. The parameters of the LEPS potential are adjusted to reproduce the *ab initio* calculation results [21, 22].

Since we describe the PES as a function of a mass-weighted coordinate, such as Z, we can observe the different shapes of the PES for different isotope combinations. In figure 1, we show the two-dimensional (2D) LEPS PESs as functions of Z and r for the case where the incident hydrogen atom impinges normal to the surface, coming directly on top of the adsorbed hydrogen atom (the coordinate X is fixed at 0.00 Å, which corresponds to the on-top site of Cu(111)). Dashed curves (from region A to C via B) correspond to the reaction path for direct abstraction reactions (e.g., ER reaction). For a gas-phase hydrogen atom of mass m_g and an adsorbed one of mass m_a, the angle ϕ subtended by the reaction path, in the asymptotic region (gas-phase hydrogen atom and hydrogen atom adsorbed on Cu(111): region A), and the r-axis is determined by $\tan \phi = \sqrt{m_g/m_a}$. This gives $\phi = 45°$ for H-on-H and D-on-D. For D-on-H, $\phi = 54.73°$, whereas $\phi = 35.26°$ for H-on-D. (Note that 'X-on-Y' indicates abstraction of Y atoms adsorbed on the surface by gas-phase X atoms.)

In figure 2, we show the 2D LEPS PESs as functions of the Z and r, for the case when the incident hydrogen atom impinging normal to the surface is at a fixed lateral distance from the adsorbed hydrogen atom (the coordinate X is fixed at 1.22 Å). Dashed curves (from region A′ to B′) correspond to the reaction path for indirect abstraction. However, the reaction does not proceed to region C′, because the state of region C′ requires very high energies (around the dissociation energy of gas-phase hydrogen molecule, $\approx$4.6 eV). Thus, the incident hydrogen atom is either scattered back to the gas phase, or trapped on the surface (where the translational energy that the incident hydrogen atom loses as a result of, e.g., diffraction corresponds to the parallel translational energy of the trapped hydrogen atom). The trapped hydrogen atom may behave as a hot atom, i.e., diffuse through the surface, react with another adsorbed hydrogen atom, then desorb as a hydrogen molecule (for example, the reaction from region B′ in figure 2 to C via B in figure 1).

In order to describe direct and indirect abstraction, it is advantageous to transform from Cartesian coordinates to reaction path coordinates [23–25]. In our calculations, we set the reaction path in the (r, Z) plane. The transformation from the Cartesian coordinates the (r, Z) to the mass-weighted reaction path coordinates (s, v) is given by
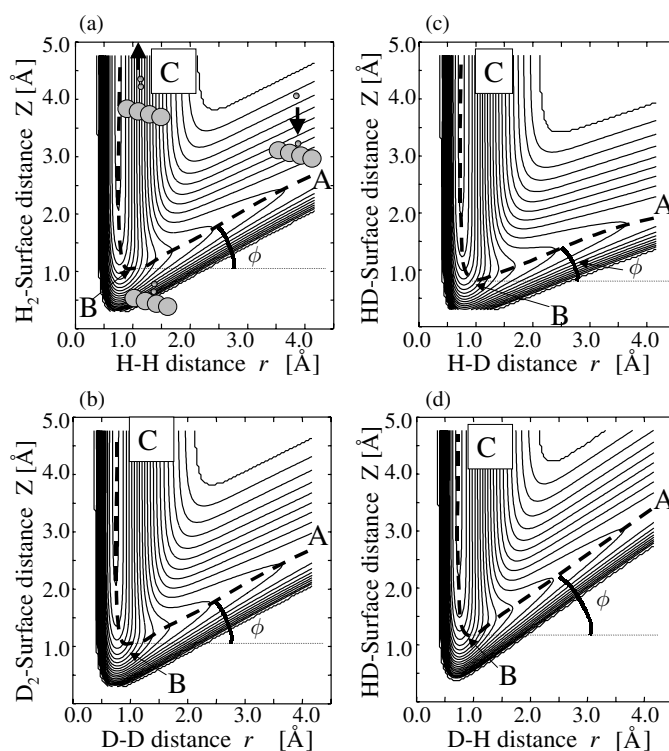
$$r = r_c(s) - v\frac{\partial z_c(s)}{\partial s} \tag{2}$$

and

$$z = z_c(s) + v\frac{\partial r_c(s)}{\partial s} \qquad \left(z = \sqrt{\frac{M}{\mu}}Z\right). \tag{3}$$

s and v are the centre-of-mass coordinates of the two hydrogen atoms along the reaction path curve, and the centre-of-mass distance of the two hydrogen atoms normal to the reaction path curve, respectively. $r_c(s)$ and $z_c(s)$ represent the reaction path curve as a function of s. As a result, we get the following final form for the Hamiltonian:

$$H = -\frac{\hbar^2}{2\mu}\left[\eta^{-1}\frac{\partial}{\partial s}\eta^{-1}\frac{\partial}{\partial s} + \eta^{-1}\frac{\partial}{\partial v}\eta\frac{\partial}{\partial v}\right] - \frac{\hbar^2}{2M}\frac{\partial^2}{\partial X^2} + V(s, v, X). \tag{4}$$

Figure 1. The PES $V(r, Z, X = 0.00$ Å) (solid curves) and the reaction path for hydrogen abstraction (dashed curves) for each isotope combination: (*a*) H-on-H, (*b*) D-on-D, (*c*) H-on-D, and (*d*) D-on-H. The energy spacing of the contour plot is 0.2 eV. The regions from A to C marked in these figures correspond to a gas-phase hydrogen atom and a hydrogen atom adsorbed on Cu(111) (A), a hydrogen molecule on Cu(111) (B), a gas-phase hydrogen molecule and Cu(111) (C). ϕ corresponds to the angle subtended by the reaction path, in the asymptotic region, and the r-axis (dotted curves).

Here, η is the Jacobian of the transformation $\eta(s, v) = 1 - vC(s)$, where $C(s)$ is the reaction path curvature. The reaction path curvature $C(s)$ is related to $r_c(s)$ and $z_c(s)$ by the equation,
$C(s) = (\mathrm{d}^2 z_c/\mathrm{d}s^2)/\sqrt{1 - (\mathrm{d}z_c/\mathrm{d}s)} = -(\mathrm{d}^2 r_c/\mathrm{d}s^2)/\sqrt{1 - (\mathrm{d}r_c/\mathrm{d}s)}$.

The $V(s, v, X)$ is the PES in the reaction path coordinate system, and we can separate the v- and X-dependences in the form

$$V(s, v, X) = V_{\mathrm{vib}}(s, v) + V_{\mathrm{cor}}(s, X). \tag{5}$$

For $V_{\mathrm{vib}}(s, v)$, we assume a harmonic-type potential:

$$V_{\mathrm{vib}}(s, v) = \tfrac{1}{2}\mu\omega(s)^2 v^2 \tag{6}$$

and

$$V_{\mathrm{cor}}(s, X) = V_0(s) + V_1(s)\cos(2\pi X/a) + [V_2(s) + V_3(s)X^2]\exp(-X^2). \tag{7}$$

$\omega(s)$ takes on the value of the frequency of vibration between an adsorbed hydrogen atom and a Cu atom at $s = \infty$, and that of the vibrational frequency of desorbing hydrogen molecules at $s = -\infty$. For $V_{\mathrm{cor}}(s, X)$, we assume a cosine function for the corrugated part of the PES, and a Gaussian function for the adsorbate part of the PES. The $V_i(s)$ ($i = 0$–3) are determined such that equation (3) fits the LEPS PES results [14, 15] (see figure 3). As can be seen in figures 1
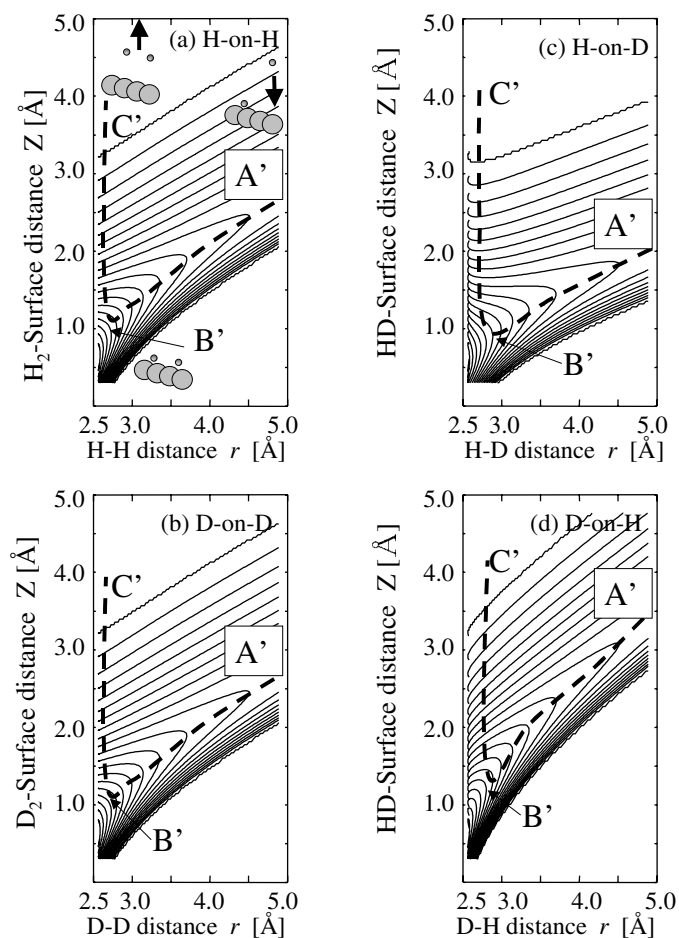
Figure 2. The PES $V(r, Z, X = 1.22 \text{ Å})$ (solid curves) and reaction path for hydrogen abstraction (dashed curves) for each isotope combination: (*a*) H-on-H, (*b*) D-on-D, (*c*) H-on-D, and (*d*) D-on-H. The energy spacing of the contour plot is 0.2 eV. The regions from A' to C' marked in these figures correspond to a gas-phase hydrogen atom and a hydrogen atom adsorbed on Cu(111) (A'), two hydrogen atoms on Cu(111) (B'), and two gas-phase hydrogen atoms and Cu(111) (C').

and 2, the behaviours of the reaction path curvature $C(s)$ and the frequency $\omega(s)$ depend on which isotopes are taken as reaction partners. In figure 4, we plot $C(s)$ and $\hbar\omega(s)$ for each isotope combination as functions of the reaction path s.

The total wavefunction is expanded in terms of one-dimensional plane waves along the X-axis and harmonic oscillator functions $\beta_n(s, v)$ along the v-axis, i.e.,

$$\Psi(s, v, X) = \sum_{m=-m_{\max}}^{m_{\max}} \sum_{n=0}^{n_{\max}} \phi_{mn}(s) \exp(-\mathrm{i}GmX)\beta_n(s, v), \tag{8}$$

where $\phi_{mn}(s)$ is the expansion coefficient of the total wavefunction along the reaction path. m is the quantum number for the centre-of-mass motion of 2H parallel to the surface, and corresponds to the diffraction channels. n is the quantum number for the vibrational motion of the product H_2. $G = 2\pi\Theta_H/a$ is the reciprocal-lattice constant, which depends on the coverage Θ_H. In this paper, we performed coupled-channel calculations for cases where the coverage $\Theta_H = 0.500$ ML.
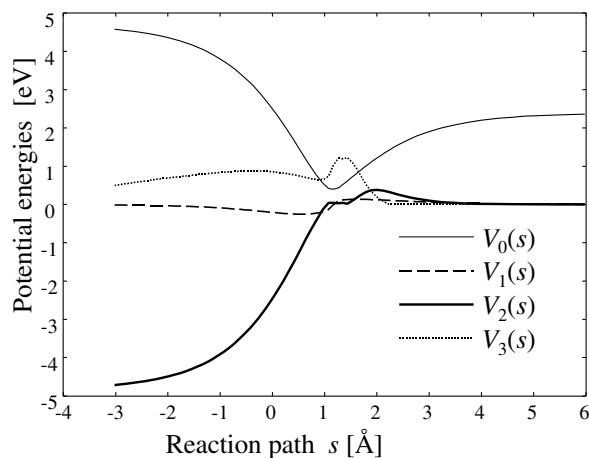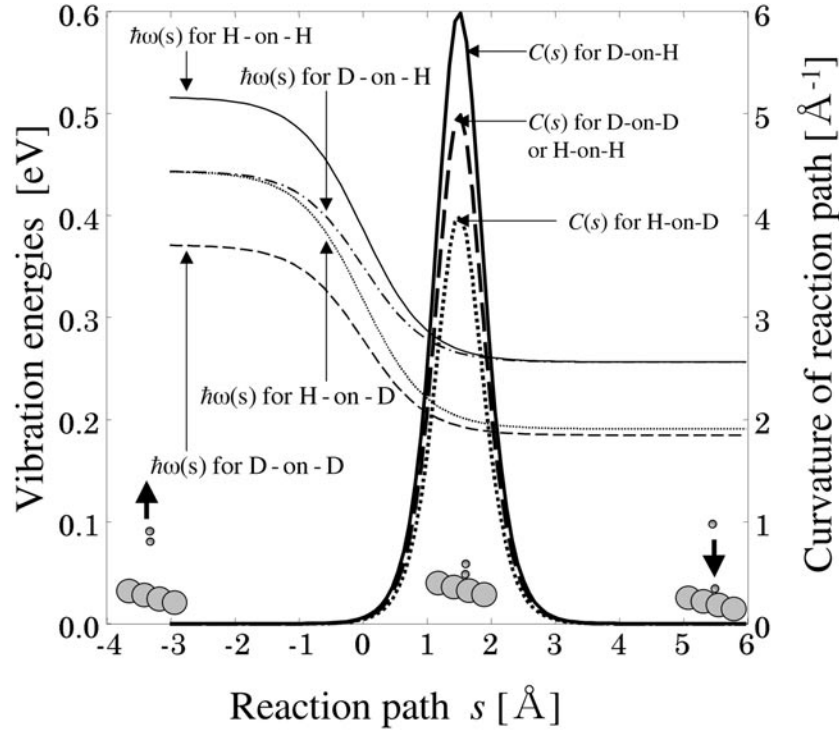
Figure 3. Coefficients of expansion of the PES $V(s, X)$ along the reaction path s, used in the present calculation. In the asymptotic region $s = \infty$, we have a gas-phase hydrogen atom and an adsorbed hydrogen atom on Cu(111). In the asymptotic region $s = -\infty$, we have a gas-phase hydrogen molecule and Cu(111). The solid curve corresponds to $V_0(s)$, the dashed curve corresponds to $V_1(s)$, the thick solid curve corresponds to $V_2(s)$, and the dotted curve corresponds to $V_3(s)$.

The basis set used in the coupled-channel calculations is determined by the incident energy $E^{\text{inci}} = 0.08$ eV and the exothermicity of this reaction (2.6 eV). The maximum numbers of channels used in the present calculations are $n_{\max} = 10$ and $m_{\max} = 60$. We carefully checked the convergence of our calculation results with maximum quantum numbers $n_{\max} = 12$ and $m_{\max} = 70$.

3. Results and discussion

We calculate the transmission coefficient $T_{n_f,m_f}^{n_i,m_i}$ and the reflection coefficient $R_{n_f,m_f}^{n_i,m_i}$ by solving the Schrödinger equation describing hydrogen abstraction from Cu(111), for incident energy of the impinging hydrogen atom $E^{\text{inci}} = 0.08$ eV. Note that n_i (n_f) and m_i (m_f) correspond to the initial (final) vibration and diffraction states of this system. Satisfaction of the unitarity requirement $\sum_{n_f,m_f} T_{n_f,m_f}^{n_i,m_i} + R_{n_f,m_f}^{n_i,m_i} = 1$ is carefully checked for all initial states. The vibrational energy of a product hydrogen molecule is given by $E_{\text{vib}}(n_f) = \hbar\omega(s = -\infty)(n_f + \frac{1}{2})$, with the vibrational energy constant $\hbar\omega(s = -\infty)$ for each isotope combination (see figure 4). The surface-parallel translational energy of a product hydrogen molecule is also given by $E_{\text{para}}(m_f) = Qm_f^2$, with the surface-parallel translational energy constant $Q = \hbar^2 G^2/2M$, where G is the reciprocal-lattice constant for Cu(111) (the surface coverage $\Theta = 0.500$ ML). Note that $Q = 1.58$ meV for H-on-H, $Q = 0.792$ meV for D-on-D, $Q = 1.06$ meV for H-on-D and D-on-H. In our calculations, we assume normal incidence of the impinging hydrogen atoms and that the adsorbed hydrogen atom is initially in the vibrational ground state (i.e., $n_i = 0$ and $m_f = 0$), for all isotope combinations.

In table 1, we show the abstraction reaction probability P_{reac}, the scattering probability P_{scat}, and the trapping probability P_{trap} for each isotope combination. The reaction probability P_{reac} and the trapping probability P_{trap} are evaluated from the transmission coefficient $T_{n_f,m_f}^{n_i,m_i}$. We can obtain the reaction probability P_{reac} by summing $T_{n_f,m_f}^{n_i,m_i}$ with the condition $E_{\text{norm}}^{\text{reac}} > 0$:

Figure 4. The reaction path curvatures and vibration frequencies along the reaction path, used in the present calculation. In the asymptotic region $s = \infty$, we have a gas-phase hydrogen atom and an adsorbed hydrogen atom on Cu(111). In the asymptotic region $s = -\infty$, we have a gas-phase hydrogen molecule and Cu(111). The solid curve corresponds to $\hbar\omega(s)$ for H-on-H, the dashed curve corresponds to $\hbar\omega(s)$ for D-on-D, the dotted curve corresponds to $\hbar\omega(s)$ for H-on-D, and the dashed-and-single-dotted curve corresponds to $\hbar\omega(s)$ for D-on-H. The thick solid curve corresponds to $C(s)$ for H-on-H and D-on-D, the thick dashed curve corresponds to $C(s)$ for H-on-D, and the thick dotted curve corresponds to $C(s)$ for D-on-H.

$$P_{\text{reac}} = \sum_{n_f=0}^{n_{\max}} \sum_{m_f=-m_{\max}}^{m_{\max}} T_{n_f,m_f}^{n_i,m_i} \qquad (E_{\text{norm}}^{\text{reac}} > 0), \tag{9}$$

where $E_{\text{norm}}^{\text{reac}} = E^{\text{inci}} - V_{\text{cor}}(s = -\infty, X) - Qm_f^2 - \hbar\omega(s = -\infty)(n_f + \frac{1}{2})$ is the normal translational energy of a product hydrogen molecule, and $V_{\text{cor}}(s = -\infty, X) \approx -2.6$ eV. Since the $V_{\text{cor}}(s, X)$ matrix has off-diagonal elements in the asymptotic region $s = -\infty$, there are some open channels in the case of $E_{\text{norm}}^{\text{reac}} < 0$. When $E_{\text{norm}}^{\text{reac}} < 0$, the impinging hydrogen atom and adsorbed hydrogen atom cannot desorb from the surface, and are trapped on the surface. We define the trapping probability P_{trap} as

$$P_{\text{trap}} = \sum_{n_f=0}^{n_{\max}} \sum_{m_f=-m_{\max}}^{m_{\max}} T_{n_f,m_f}^{n_i,m_i} \qquad (E_{\text{norm}}^{\text{reac}} < 0). \tag{10}$$

In this case, the trapped hydrogen atom diffuses across the surface as a hot atom with an energy Qm_f^2. The scattering probability P_{scat} is evaluated from the reflection coefficient $R_{n_f,m_f}^{n_i,m_i}$:

$$P_{\text{scat}} = \sum_{n_f=0}^{n_{\max}} \sum_{m_f=-m_{\max}}^{m_{\max}} R_{n_f,m_f}^{n_i,m_i} \qquad (E_{\text{norm}}^{\text{scat}} > 0), \tag{11}$$

Table 1. The abstraction reaction probability P_{reac}, the atom scattering probability P_{scat}, and the atom trapping probability P_{trap} for each isotope combination.

	P_{reac}	P_{scat}	P_{trap}
H-on-H	0.594	0.199	0.204
D-on-D	0.742	0.158	0.095
H-on-D	0.640	0.178	0.179
D-on-H	0.533	0.315	0.151

Table 2. The mean vibrational energy $\langle E_{\text{vib}}\rangle$, the mean normal translational energy $\langle E_{\text{norm}}\rangle$, and the mean parallel translational energy $\langle E_{\text{para}}\rangle$ of product hydrogen molecules for each isotope combination.

	$\langle E_{\text{vib}}\rangle$ (eV)	$\langle E_{\text{norm}}\rangle$ (eV)	$\langle E_{\text{para}}\rangle$ (eV)
H-on-H	0.525	0.914	0.251
D-on-D	0.713	1.03	0.314
H-on-D	0.573	1.03	0.191
D-on-H	0.498	0.807	0.190

where $E_{\text{norm}}^{\text{scat}} = E^{\text{inci}} - V_{\text{cor}}(s = +\infty, X) - Qm_f^2 - \hbar\omega(\infty)(n_f + \frac{1}{2})$ is the normal translational energy of a scattered hydrogen atom, and $V_{\text{cor}}(s = +\infty, X) \approx 0$ eV. Since the $V_{\text{cor}}(s, X)$ matrix has no off-diagonal elements in the asymptotic region $s = +\infty$, there are no open channels in the case of $E_{\text{norm}}^{\text{scat}} < 0$.

In order to investigate the energy distribution of product hydrogen molecules in hydrogen abstraction reactions, we calculate the mean vibrational and normal/parallel translational energy of product hydrogen molecules. We give these energies as follows:

$$\langle E_{\text{vib}}\rangle = \sum_{n_f=0}^{n_{\max}} E_{\text{vib}}(n_f) \sum_{m_f=-m_{\max}}^{m_{\max}} T_{n_f,m_f}^{n_i,m_i}, \tag{12}$$

$$\langle E_{\text{norm}}\rangle = \sum_{n_f=0}^{n_{\max}} \sum_{m_f=-m_{\max}}^{m_{\max}} E_{\text{norm}}^{\text{reac}} T_{n_f,m_f}^{n_i,m_i}, \tag{13}$$

and

$$\langle E_{\text{para}}\rangle = \sum_{m_f=-m_{\max}}^{m_{\max}} E_{\text{para}}(m_f) \sum_{n_f=0}^{n_{\max}} T_{n_f,m_f}^{n_i,m_i}. \tag{14}$$

In table 2, we show $\langle E_{\text{vib}}\rangle$, $\langle E_{\text{norm}}\rangle$ and $\langle E_{\text{para}}\rangle$ for each isotope combination.

4. Discussion

From P_{reac}, we can estimate the reaction cross sections of hydrogen abstraction from Cu(111) $\sigma_{\text{reac}} = P_{\text{reac}}S$, where $S = 9.24$ Å^2 is the area that one adsorbed hydrogen atom occupies on Cu(111) for the case of $\Theta = 0.500$ ML. We obtain reaction cross section $\sigma_{\text{reac}} = 5.49$ Å^2 for H-on-H, $\sigma_{\text{reac}} = 6.86$ Å^2 for D-on-D, $\sigma_{\text{reac}} = 5.91$ Å^2 for H-on-D, and $\sigma_{\text{reac}} = 4.92$ Å^2 for D-on-H. The experimental estimate of the reaction cross section is $\approx 5.2 \pm 1.3$ Å^2. Thus, our calculation results quantitatively agree with the experimental results, and our quantum dynamics model, which considers both the direct and the indirect process, describes the hydrogen abstraction dynamics quite well.

By comparing P_{reac} for each isotope combination, we can observe the following results in hydrogen abstraction reactions. First, D abstraction is easier (D-on-D and H-on-D) as

compared to H abstraction (H-on-H and D-on-H). On the other hand, the atom scattering probability P_{scat} is larger for H abstraction as compared to D abstraction. This is due to the difference in zero-point energies of H–Cu vibration. Since D–Cu vibration is softer as compared to H–Cu vibration (here, 'soft' means that the vibrational energy constant of D–Cu vibration $\hbar\omega(\infty)$ is smaller than that of H–Cu vibration), energy transfer from an impinging D to the adsorbed H is more effective than energy transfer from an impinging H to the adsorbed D when two hydrogen atoms collide. Thus, breaking of the hydrogen–Cu bond and desorbing of hydrogen molecules from the surface effectively occur for the D-adsorbed surface.

Second, the abstraction probabilities depend on the curvature of the reaction path $C(s)$. Comparing P_{reac} for H-on-H (0.594) and D-on-H (0.533), we can say that the abstraction reaction easily occurs when the curvature of the reaction path $C(s)$ is not so large (the maximum value of $C(s)$ is 5.00 Å^{-1} for H-on-H and 6.00 Å^{-1} for D-on-H; see figure 4). Because the coupling between the Z and r is too strong when $C(s)$ is large, therefore, energy transfer from impinging hydrogen atom to adsorbed hydrogen atom is suppressed.

Third, H is easily trapped compared with D. The atom trapping probability P_{trap} is larger for the case of an H atom impinging (0.204 for H-on-H and 0.179 for H-on-D) than that for the case of D impinging (0.0945 for D-on-D and 0.151 for D-on-H). The light H is easier to trap on the surface due to the large zero-point energy of H–Cu vibration.

In table 2, we see that the mean normal translational and vibrational energies for H-on-D are larger than those for D-on-H, while the mean parallel translational energy for D-on-H is comparable with that for H-on-D. This implies that, in spite of the small reaction probability for D-on-H, the indirect process does not decrease in frequency of occurrence. Thus, the decrease of the abstraction reaction probability for D-on-H is mainly due to the decrease in frequency of occurrence of direct processes in hydrogen abstraction reactions. We conclude that this is a manifestation of the *steering* of the incident hydrogen atom in the abstraction reaction. *Steering* is the dynamical repositioning of the incident hydrogen atom on the corrugated surface, to seek pathways of the lowest potential energy. Since interaction between a gas-phase hydrogen atom and a hydrogen atom adsorbed on Cu(111) is repulsive, at the initial stage of a hydrogen atom impinging to the surface, the hydrogen atom approaching the surface just above the adsorbed atom may steer and move parallel to the surface to avoid it. Because D is slower than H, due to the heavier mass of D for the same incident energy, D has more time to complete *steering* as compared to H. Therefore, *steering* will be more effective with D than H, and D can easily avoid the high-energy parts of the PES (i.e., D can easily avoid direct interaction with an adsorbed hydrogen atom as compared with H). This leads to the decrease in frequency of occurrence of the direct process in hydrogen abstraction for D-on-H as compared with H-on-D.

5. Summary

In this paper, we investigate and discuss the dynamics of hydrogen abstraction from Cu(111) by performing quantum dynamics calculations, and including both the *direct* (the impinging hydrogen atom directly abstracts an adsorbed hydrogen atom) and *indirect* (the impinging hydrogen atom diffuses across the surface before it abstracts an adsorbed hydrogen atom) processes for hydrogen abstraction. We investigate isotope effects on the direct and indirect process of hydrogen abstraction reactions. Our calculation results show strong isotope dependence of the total reaction, scattering, and trapping probabilities, and the calculated reaction cross sections quantitatively agree with the experimental estimations. Furthermore, comparing the mean vibrational and normal/parallel translational energies for H-on-D and D-on-H, we conclude that the direct process is more dominant for H-on-D as compared with D-on-H. Since dynamical *steering* is more effective with D than H, D can easily avoid direct interaction with an adsorbed hydrogen atom as compared with H.

In the present study, we employed an approximate treatment for the surface-parallel motion and rotational motion of a hydrogen molecule. In our future work, we will go beyond an approximate treatment, and also investigate the hydrogen abstraction dynamics on a more realistic metal surface to obtain a more detailed understanding for the selectivity of *direct/indirect* reaction and the energy distribution of product hydrogen molecules in the dynamics of hydrogen abstraction from metal and semiconductor surfaces.

Acknowledgments

References

[1] Rettner C T 1992 *Phys. Rev. Lett.* **69** 383
[2] Rettner C T and Auerbach D J 1996 *J. Chem. Phys.* **104** 2732
[3] Kratzer P and Brenig W 1991 *Surf. Sci.* **254** 275
[4] Jackson B and Persson M 1992 *J. Chem. Phys.* **96** 2378
[5] Kammler Th, Wehner S and Küppers J 1995 *Surf. Sci.* **339** 125
[6] Eilmsteiner G and Winkler A 1996 *Surf. Sci.* **366** L750
[7] Buntin S A 1997 *Chem. Phys. Lett.* **278** 71
[8] Boh J, Eilmsteiner G, Rendulic K D and Winkler A 1998 *Surf. Sci.* **395** 98
[9] Kammler Th, Vellianitis D K and Küppers J 2000 *Surf. Sci.* **460** 91
[10] Okada M, Moritani K, Nakamura M, Kasai T and Murata Y 2000 *Chem. Phys. Lett.* **323** 586
[11] Kim J Y and Lee J 2000 *J. Chem. Phys.* **113** 2856
[12] Persson M and Jackson B 1995 *J. Chem. Phys.* **102** 1078
[13] Dai J and Light J C 1999 *J. Chem. Phys.* **110** 6511
[14] Caratzoulas S, Jackson B and Persson M 1997 *J. Chem. Phys.* **107** 6420
[15] Persson M, Strömquist J, Bengtsson L, Jackson B, Shalashilin D V and Hammer B 1999 *J. Chem. Phys.* **110** 2240
[16] Shalashilin D V, Jackson B and Persson M 1999 *J. Chem. Phys.* **110** 11 038
[17] Jackson B and Lemoine D 2001 *J. Chem. Phys.* **114** 474
[18] Kratzer P 1997 *J. Chem. Phys.* **106** 6752
[19] Rutigliano M, Cacciatore M and Billing G D 2001 *Chem. Phys. Lett.* **340** 13
[20] McCreery J H and Wolken G Jr 1975 *J. Chem. Phys.* **63** 2340
[21] Hammer B, Scheffler M, Jacobsen K W and Nørskov J K 1994 *Phys. Rev. Lett.* **73** 1400
[22] Strömquist J, Bengtsson L, Persson M and Hammer B 1998 *Surf. Sci.* **397** 382
[23] Miura Y, Kasai H, Diño W A and Okiji A 2000 *J. Phys. Soc. Japan* **69** 3878
[24] Miura Y, Kasai H, Diño W A and Okiji A 2002 *J. Phys. Soc. Japan* **71** 222
[25] Miura Y, Kasai H and Diño W A 1999 *J. Phys. Soc. Japan* **68** 887